JOURNAL OF COMPUTATIONAL PHYSICS 95, 175–194 (1991)

Computations of Transitions and Taylor Vortices in Temporally Modulated Taylor–Couette Flow

CARLO F. BARENGHI

Department of Mathematics and Statistics, Division of Applied Mathematics, The University, Newcastle upon Tyne NE1 7RU, England

Received May 30, 1989; revised January 6, 1990

Numerical methods are presented to study the temporally modulated Taylor–Couette flow problem. The first method uses Floquet theory to examine the transition from azimuthal flow to axisymmetric oscillating Taylor vortices. The second method uses a spectral initial value code to investigate the nonlinear development of these vortices. The properties of stability and convergence of the methods are discussed. To illustrate the significance of these methods new results about the generation of a vortex pair and the subharmonic response of stretched vortices are also presented. © 1991 Academic Press, Inc.

1. INTRODUCTION

(a) *The Modulated Taylor–Couette Problem*

The physical problem which gives rise to the calculations and the numerical methods described in this paper is temporally modulated Taylor–Couette flow [1, 2]. Our concern is the motion of an incompressible viscous fluid which is contained in the gap between two concentric cylinders which rotate at assigned angular velocities. We assume for the sake of simplicity that the outer cylinder is fixed and distinguish between a "steady" and a "modulated" Taylor–Couette problem.

In the "steady" Taylor–Couette problem the velocity of the inner cylinder, measured by the Reynolds number Re_1, is kept constant in time. If Re_1 is small enough the fluid exhibits steady azimuthal motion, called Couette flow. If Re_1 is increased above a critical value Re_{1C} then Couette flow becomes unstable and a transition occurs: the radial and axial velocity components become different from zero and the flow takes the form of axisymmetric toroidal vortices, called Taylor vortices.

In the "modulated" Taylor–Couette problem the velocity of the inner cylinder is not constant but varies periodically in time with assigned frequency and amplitude, i.e., $\mathrm{Re}_1(t) = \overline{\mathrm{Re}}_1[1 + \varepsilon_1(\sin(\omega_1 t)]$. Typically $\varepsilon_1 < 1$ is chosen. If $\overline{\mathrm{Re}}_1$ is sufficiently small the flow is again purely azimuthal, in the form of a spatially damped oscillating viscous wave. If $\overline{\mathrm{Re}}_1$ is larger than a critical value $\overline{\mathrm{Re}}_{1C}$ then the viscous wave loses stability and axisymmetric vortex motion onsets. Two interesting questions arise. The first is whether the modulation makes the flow more or less stable to the onset of vortices than the steady case. This leads to the study of the

0021-9991/91 $3.00

581/95/1-12

threshold shift $r = (\overline{\mathrm{Re}}_{1C} - \mathrm{Re}_{10})/\mathrm{Re}_{10}$ as a function of amplitude ε_1 and frequency ω_1: at high frequency only a thin layer of fluid close to the inner cylinder is affected, while at low frequency the Stokes layer is large and we expect that the modulation has significant effects. The second question concerns the nonlinear development of the vortex flow above onset. The purpose of this paper is to describe the numerical tools used in Ref. [3] to answer these questions, a Floquet theory to study the onset of vortices, and an initial value code to investigate the nonlinear flow.

(b) *Previous Work and Plan of This Paper*

In a recent paper [3] we have argued that in the modulated Taylor–Couette problem there are disturbances which cause the bifurcation from Couette flow to Taylor vortices to become imperfect: for example, thermal differences across the gap, geometrical variations of the radii of the cylinders along their length, and the flakes used for the flow visualization. These imperfections are almost irrelevant in the steady state problem but have important consequences at low frequency modulation, because they prevent the radial and axial velocity components from decaying to very small values during the part of the cycle in which the Reynolds number is below critical. Our analysis, based on an amplitude equation approach, suggested an explanation for the disagreement that previously existed in the literature. On one hand there are the experiments of Thomson [4] and of Walsh and Donnelly [5] in wich very large threshold shifts $r = O(\varepsilon_1)$ were measured, showing that the modulation strongly destabilizes the flow; the same result was predicted by the linear stability theory of Carmi and Tustaniwskyj [6]. On the other hand, Hall [7] showed analytically, by means of expansions in both small frequency and small amplitude of modulation, that in the narrow gap limit $\overline{\mathrm{Re}}_{1C}$ is very close to Re_{10} and $r = O(\varepsilon_1^2)$. In support of Hall's theory is the narrow gap limit computation of Riley and Laurence [8] and, more recently, the theory of Kuhlmann *et al.* [9] and the experiment of Ahlers [10].

We found [3] that in a perfect bifurcation the destabilization is a small $O(\varepsilon_1^2)$ effect, but a low enough frequency the imperfections take over. No matter how well the experimenter tries to control the imperfections, there exists a cutoff frequency below which these become significant and cause the threshold shift to become large, i.e., $r = O(\varepsilon_1)$. Calculation of this cutoff frequency showed quantitative agreement with the experimental value. We also modelled the imperfections by introducing suitable modifications in the initial value code which we describe in this paper and confirmed the result of the amplitude equation. The disagreement between the experiment of Walsh and Donnelly [5] and the recent work of Ahlers [10] is explained by the fact that in the latter the frequency of modulation was above the cutoff below which the bifurcation becomes imperfect, whereas Walsh and Donnelly used a lower (dimensionless) frequency.

To clarify the picture completely one has still to understand why, within the framework of the perfect bifurcation, the stability approach of Carmi and Tustaniwskyj [6] predicted too large threshold shifts at low frequency of modulation. For this purpose we have developed a linear stability theory around an

oscillating state (Floquet theory). Following Carmi and Tustaniwskyj, our theory does not assume the narrow gap limit, so that precise comparison with experimental data is possible. Our results [3] are in good agreement with the calculations of Hall [7] and Kuhlman *et al.* [9], with the experiment of Ahlers [10] and with some recent work of Walsh and Donnelly [11] in which it was discovered that the modulation of the outer cylinder strongly stabilizes the flow.

The present paper contains a description of the numerical methods used in [3] to implement the Floquet theory; particular attention has been given to the tests of the code and the comparison with the work of Carmi and Tustaniwsky. The most likely source of the disagreement is found to be the time stepping.

The other numerical methods which we shall describe in this paper refer to an initial value code used in Ref. [3] to study the nonlinear oscillating Taylor vortices. A number of numerical calculations have been performed in the past to study the steady axisymmetric Taylor–Couette problem. Meyer [12], Rogers and Beard [13], and Meyer–Spasche and Keller [14] used finite differences in the radial direction and Fourier expansions axially. Jones [15] considered the more general nonaxisymmetric problem and compared the relative merits of a full spectral approach in both radial and axial directions with methods which are spectral in one direction and finite difference in the other. Initial value codes for nonaxisymmetric Taylor vortices based on spectral methods have been developed by Moser, Moin, and Leonard [16] and Marcus [17]. Marcus investigated the use of a fractional time step scheme using Chebyshev polynomials in which each time step was split into three independent corrections for the nonlinear terms, the pressure and the viscous term. The time splitting method was used successfully in cylindrical pipe flow [18], but when calculating Taylor–Couette flow problems arose from imposing the continuity constraint on the second intermediate step. These problems were eliminated by Marcus [17] by using a Green's function method. Moser, Moin, and Leonard [16] used spectral expansions which inherently satisfied the boundary conditions and the continuity equation. The resulting banded matrices were solved at each time step. A method for temporally modulated axisymmetric Taylor flow, based on a finite difference simulation of the Navier–Stokes equation, was developed by Kuhlmann *et al.* [9]. The method which we shall present in this paper to study temporally modulated Taylor–Couette flow is based on Chebyshev–Fourier spectral expansions. The matrices which drive the evolution can be computed in advance of the time integration.

The plan of the paper is the following. In Section 2 we shall introduce the notation and the equations of motion in their dimensionless form. In Section 3 we shall describe the initial value code which we have developed to solve these equations, together with a discussion of its properties of stability and convergence. In Section 4 we shall present the Floquet theory, study the effect of changing the mode truncation and the time step and make comparison with Carmi and Tustaniwskyj's work [6]. In Section 5, to illustrate the significance of our numerical methods, we shall present some new results: the use of the time modulation to study the generation of a vortex pair and the subharmonic response of stretched vortices.

2. The Equations of Motion

Let us consider a fluid of given density ρ and kinematic viscosity ν which is confined between two infinitely long concentric cylinders. The inner and the outer cylinders have radii R_1 and R_2, respectively. In the previous section we restricted the discussion to modulations of the inner cylinder with the outer cylinder at rest, but now we consider the more general situation in which both cylinders rotate at assigned angular velocities $\Omega_i(t) = \bar{\Omega}_i(1 + \varepsilon_i \sin \omega_i t)$, $i = 1, 2$. The flow is described by the incompressible Navier–Stokes equations

$$\partial \mathbf{u}/\partial t + (\mathbf{u} \cdot \nabla)\,\mathbf{u} = -1/\rho\, \nabla p + \nu\, \nabla^2 \mathbf{u} \tag{2.1}$$

$$\nabla \cdot \mathbf{u} = 0, \tag{2.2}$$

where p is the pressure and the velocity field $\mathbf{u}$ has components (u_r, u_φ, u_z) in cylindrical coordinates (r, φ, z). The nonslip boundary conditions are $u_r(r = R_1) = u_r(r = R_2) = u_z(r = R_1) = u_z(r = R_2) = 0$, $u_\varphi(r = R_1) = \Omega_1(t)\, R_1$, and $u_\varphi(r = R_2) = \Omega_2(t)\, R_2$.

The experimental evidence shows that modulated Taylor flow is axisymmetric after the onset. We seek solutions of (2.1), (2.2) which do not depend on the angle φ and introduce the stream function Ψ

$$u_r = -1/r\, \partial \Psi/\partial z, \qquad u_z = 1/r\, \partial \Psi/\partial r \tag{2.3}$$

which automatically guarantees that (2.2) is satisfied, and the potential vorticity $Z = (\operatorname{curl} \mathbf{u})_\varphi / r$,

$$Z = -\frac{1}{r}\frac{\partial}{\partial r}\left(\frac{1}{r}\frac{\partial \Psi}{\partial r}\right) - \frac{1}{r^2}\frac{\partial^2 \Psi}{\partial z^2}. \tag{2.4}$$

It is convenient to write the total azimuthal velocity as $u_\varphi = u_\varphi^0 + v$, where u_φ^0 is the instantaneous Couette flow $u_\varphi^0 = a(t)\, r + b(t)/r$, with $a(t)$ and $b(t)$ determined by the boundary conditions:

$$a(t) = \frac{R_2^2 \Omega_2(t) - R_1^2 \Omega_1(t)}{R_2^2 - R_1^2}, \qquad b(t) = \frac{R_2^2 R_1^2 [\Omega_1(t) - \Omega_2(t)]}{R_2^2 - R_1^2}. \tag{2.5}$$

In this way the boundary conditions for v are simply $v(r = R_1) = v(r = R_2) = 0$ and the boundary conditions for Ψ are chosen to be $\Psi(r = R_1) = \Psi(r = R_2) = \Psi(\partial \Psi/\partial r)(r = R_1) = (\partial \Psi/\partial r)(r = R_2) = 0$.

We now make the equations of motion dimensionless. Let $\delta = R_2 - R_1$ be the gap width and $\eta = R_1/R_2$ the radius ratio. We introduce the following variables $t \to \nu/\delta^2 t$, $r \to (r - R_1)/\delta = x$, $z \to z/\delta = \zeta$ and fields $v \to v/\delta v$, $Z \to \nu/R_2 \delta^2 Z$, $\Psi \to \nu R_2 \Psi$ and $u_\varphi^0 \to \nu/\delta u_\varphi^0$.

The dimensionless velocities of the inner and the outer cylinder are the Reynolds numbers $\mathrm{Re}_i(t) = \Omega_i(t)\, R_i \delta/\nu = \overline{\mathrm{Re}}_1(1 + \varepsilon_i \sin \omega_i t)$, $i = 1, 2$, where ω_i are now

dimensionless frequencies and $T_i = 2\pi/\omega_i$ are the respective periods. It is also common in the literature to use the Taylor number $\mathrm{Ta} = 2\Omega_1^2 \delta^4(\eta^2 - \mu)/[(1-\eta^2)\, \nu^2]$ together with the ratio $\mu = \Omega_2/\Omega_1$.

We conclude that the dimensionless axisymmetric incompressible Navier–Stokes equations for Z, v, and φ and the boundary conditions are

$$\partial Z/\partial t = L_1(Z) + N_1(Z, v, \Psi) \tag{2.6}$$

$$\partial v/\partial t = L_2(v) + N_2(v, \Psi) + F(t) \tag{2.7}$$

$$Z - L_3(\Psi) = 0 \tag{2.8}$$

$$v = \Psi = \partial\Psi/\partial x = 0 \qquad \text{at } x = 0 \text{ and } x = 1. \tag{2.9}$$

L_1, L_2, and L_3 are linear operators defined by

$$L_1 = \partial^2/\partial x^2 + 3(1-\eta)/s\, \partial/\partial x + \partial^2/\partial\zeta^2 \tag{2.10}$$

$$L_2 = \partial^2/\partial x^2 + (1-\eta)/s\, \partial/\partial x - (1-\eta)^2/s^2 + \partial^2/\partial\zeta^2 \tag{2.11}$$

$$L_3 = -1/s^2\, \partial^2/\partial x^2 + (1-\eta)/s^3\, \partial/\partial x - 1/s^2\, \partial^2/\partial\zeta^2, \tag{2.12}$$

where $s = (1-\eta)\, x + \eta$. N_1 and N_2 are nonlinear operators defined by

$$N_1(Z, v, \Psi) = 2(1-\eta)/s^2\, (u_\varphi^0 + v)\, \partial v/\partial\zeta - 1/s\, \partial(\Psi, Z)/\partial(x, \zeta) \tag{2.13}$$

$$N_2(\Psi, v) = -1/s\, \partial(\Psi, v)/\partial(x, \zeta) + (1-\eta)/s\, (v/s + 2A)\, \partial\Psi/\partial\zeta, \tag{2.14}$$

where we have used the definition $\partial(f, g)/\partial(x, y) = \partial f/\partial x\, \partial g/\partial y - \partial f/\partial y\, \partial g/\partial x$; the instantaneous Couette flow is $u_\varphi^0 = A(t)\, s + B(t)/s$ with

$$A(t) = \frac{[\mathrm{Re}_2(t) - \eta\, \mathrm{Re}_1(t)]}{(1-\eta^2)}, \qquad B(t) = \frac{\eta[\mathrm{Re}_1(t) - \eta\, \mathrm{Re}_2(t)]}{(1-\eta^2)}. \tag{2.15}$$

Finally $F(t)$ is a known forcing term

$$F(t) = (-\omega_1 \varepsilon_1 \overline{\mathrm{Re}}_1(\eta/s - \eta s)\cos(\omega_1 t) - \omega_2 \varepsilon_2 \overline{\mathrm{Re}}_2(s - \eta^2/s)\cos(\omega_2 t))/(1-\eta^2). \tag{2.16}$$

The initial value problem (2.6) to (2.9) is completely specified by assigning the radius ratio η, the wavenumber α, the parameters $\overline{\mathrm{Re}}_i$, ε_i, ω_i $(i = 1, 2)$ which determine the Reynolds numbers as a function of time, and the initial conditions for Z, v, and Ψ.

For comparison with experimental data we often choose $\alpha = 3.13$, close to the wavenumber of the first mode to become unstable in the steady Taylor–Couette problem: there is in fact experimental evidence that the wavenumber does not change significantly in the modulated case. This value of α corresponds to a Taylor vortex cell of wavelength $\lambda = 2\pi/\alpha$ almost equal to twice the gap width. The cell

consists of a pair of vortices rotating in opposite directions. So as to make comparisons with the work of Carmi and Tustaniwskyj [6] we often adopt their choice of the geometrical factor $\delta/R_1 = 0.444$, i.e., radius ratio $\eta = 0.693$.

3. The Initial Value Code

In this section we describe the initial value code developed to solve Eq. (2.6) to (2.9). It is known that in the solution of similar equations [19] there is the difficulty of avoiding the numerical instability associated with the radial diffusion. The linear operators L_1, L_2, and L_3 must be treated implicitly: we use the second-order accurate Crank–Nicholson method. For the nonlinear operators N_1 and N_2 we use the explicit Adams–Bashforth second-order method. The external force $F(t)$ is integrated exactly. The relation between Z and φ and the boundary conditions are enforced at each time step. Let the subscript n denote any variable at time $t^n = n\,\Delta t$, where Δt is the time step. We have then

$$\left(1-\frac{\Delta t}{2}L_1\right)Z^{n+1}=\left(1+\frac{\Delta t}{2}L_1\right)Z^n + \frac{\Delta t}{2}\left(3N_1(v^n, \Psi^n, Z^n)-N_1(v^{n-1}, \Psi^{n-1}, Z^{n-1})\right) \tag{3.1}$$

$$\left(1-\frac{\Delta t}{2}L_2\right)v^{n+1}=\left(1+\frac{\Delta t}{2}L_2\right)v^{n+1} + \frac{\Delta t}{2}\left(3N_2(v^n, \Psi^n)-N_1(v^{n-1}, \Psi^{n-1})\right)+H \tag{3.2}$$

$$Z^{n+1}-L_3\Psi^{n+1}=0 \tag{3.3}$$

$$\Psi^{n+1}=0 \qquad \text{at} \quad x=0 \text{ and } 1 \tag{3.4}$$

$$\partial\Psi^{+1}/\partial x=0 \qquad \text{at} \quad x=0 \text{ and } 1 \tag{3.5}$$

$$v^{n+1}=0 \qquad \text{at} \quad x=0 \text{ and } 1, \tag{3.6}$$

where

$$H=-\frac{\varepsilon_1\overline{\mathrm{Re}}_1}{(1-\eta^2)}(\eta/s-\eta s)\left[\sin(\omega_1 t^{n+1})-\sin(\omega_1 t^n)\right] - \frac{\varepsilon_2\overline{\mathrm{Re}}_2}{(1-\eta^2)}(s-\eta^2/s)\left[\sin(\omega_2 t^{n+1})-\sin(\omega_2 t^n)\right]. \tag{3.7}$$

We expand Z, v, and Ψ over truncated Chebyshev–Fourier sums

$$Z(x, \zeta, t^n) = \sum_{m=1}^{m=NF} \sum_{k=1}^{k=NC} Z^n_{mk} \sin(m\alpha\zeta)\, T^*_{k-1}(x) \tag{3.8}$$

$$\Psi(x, \zeta, t^n) = \sum_{m=1}^{m=NF} \sum_{k=1}^{k=NC+2} \Psi^n_{mk} \sin(m\alpha\zeta)\, T^*_{k-1}(x) \tag{3.9}$$

$$v(x, \zeta, t^n) = \sum_{m=1}^{m=NF+1} \sum_{k=1}^{k=NC} v^n_{mk} \cos((m-1)\,\alpha\zeta)\, T^*_{k-1}(x). \tag{3.10}$$

Here $T^*_k(x)$ is the kth modified Chebyshev polynomial defined in the interval $0 \leqslant x \leqslant 1$. At time t^n the solution of the Navier–Stokes equations is represented by the $N = NC * NF + NC * (NF+1) + (NC+2) * NF$ coefficients Z^n_{mk}, v^n_{mk}, and Ψ^n_{mk}. N equations are needed for these coefficients.

Equations (3.1) and (3.2) and (3.3) are evaluated respectively at $NC+2$, $NC-2$, and NC points in the radial direction x. A set of M such collocation points is defined as $x_m = \frac{1}{2}[1 + \cos(m\pi/(M+1))]$, $m = 1, ..., M$. Then in each equation and boundary condition we set the coefficient of each Fourier mode $\cos(m\alpha\zeta)$ or $\sin(m\alpha\zeta)$ equal to zero. Before doing this, however, we have to rearrange the nonlinear quantities N_1 and N_2 and express them as Fourier sums; for example, a nonlinear term of the form $[\sum_{m=1}^{m=M} a_m(x) \sin(m\alpha\zeta)]$ times $[\sum_{m=1}^{m=M} b_m(x) \cos(m\alpha\zeta)]$ can be written as $[\sum_{m=1}^{m=M} c_m(x) \sin(m\alpha\zeta)]$, where the new coefficients $c_m(x)$ can be easily obtained from $a_m(x)$ and $b_m(x)$. Higher order terms, the first of which is proportional to $\sin(M+1)\,\alpha\zeta$, are ignored. In this way we obtain respectively $NF * (NC-2)$, $(NF+1) * (NC-2)$, $NF * (NC+2)$, $2 * NF$, $2 * NF$, and $2 * (NF+1)$ relations from (3.1), (3.2), (3.3), (3.4), (3.5), and (3.6) and the total number of equations equals the total number of unknowns.

Equations (3.1) to (3.6) can be written in matrix form

$$PX^{n+1} = QX^n + \Delta t/2[3Y^n - Y^{n-1}] + H^n, \tag{3.11}$$

where P and Q are square matrices of size N which depend on n, α, Δt, NC, and NF but are independent of time and of the Reynolds numbers. X^n is a vector of length N which contains the Chebyshev–Fourier coefficients of the fields Z, v, and Ψ at time t^n. Y^n is a vector of length N which depends nonlinearly on in Z, v, and Ψ at time t^n, and H^n is a known vector of length N which depends on time t^n. The algorithm for the initial value code is then

$$W = \frac{\Delta t}{2}(3Y^n - Y^{n-1}) + H^n \tag{3.12}$$

$$X^{n+1} = (P^{-1} * Q)\, X^n + (P^{-1})\, W. \tag{3.13}$$

The matrices $P^{-1} * Q$ and P^{-1} are computed in advance of the time integration and are stored in files. Since each time step requires the knowledge of the state of

the system X at two previous times, we use Euler's method to compute X^{n+1}, i.e., $\Delta t/2(3Y^n - Y^{n-1})$ in (3.12) is replaced by $\Delta t\, Y^n$. At each successive step first one finds the nonlinear terms Y^n and Y^{n-1} and the known force H^n, which together form the vector W. Then the desired vector X^{n+1} is obtained from (3.13) by summing together the results of two multiplications of a precomputed matrix times a vector. A major time saving factor is that the matrices $P^{-1} * Q$ and P^{-1} have a structure with many empty blocks; for example, $P^{-1} * Q$ has only $(2NF+1)\,NC * NC + NF * NC * (NC+2)$ nonzero elements instead of N^2.

The starting condition X^0 for the initial value code can be obtained in a number of ways. Typically one uses an existing vector X which was stored at the end of a previous run at the same or at different Reynolds number. One can also use a rough guess for X corresponding to $v = \sin \pi x$ and $\Psi = x^2(x-1)^2$. A third way is the following: we have developed an independent spectral code to study the linear stability of steady Couette flow. We do not describe this linear code here because it is similar to a method already published [20]. The eigenfunctions corresponding to a chosen eigenvalue obtained from the linear code can be used, together with an arbitrary amplitude, as starting condition X^0.

Direct calculation of the eigenvalues of the matrix $P^{-1} * Q$ confirms that all have magnitude less than one, so our method is linearly stable and does not suffer from the numerical instability associated with the diffusion operator mentioned before. What limits the size of the time step is the Courant instability of the nonlinear part; typically in the range of interest of the parameters we find instability for $\Delta t > 0.02$, and the actual Δt which we use to calculate modulated flows is much smaller to provide us with the desired accuracy.

A number of tests against known results have been performed:

(1) *Growth rates and converges in Δt.* We use the steady state linear stability program just mentioned to compute the growth rate σ_0 at given η, α, and Re_1. We

TABLE I

The Growth Rate σ Computed by the Initial Value Code as a Function of the Time Step Δt at $\delta/R_1 = 0.444$, $\alpha = 3.13$, $\mathrm{Re}_1 = 80$ with $NC = 15$ Chebyshev Polynomials

Δt	$(\sigma - \sigma_0)/\sigma_0 \times 100$
0.01	-0.574×10^{-1}
0.005	-0.144×10^{-1}
0.002	-0.230×10^{-2}
0.001	-0.576×10^{-3}
0.0005	-0.144×10^{-3}
0.0002	-0.231×10^{-4}
0.0001	-0.586×10^{-5}

Note. $\sigma_0 = 0.430108693$ is the growth rate obtained from the steady state linear stability code.

take the resulting eigenfunction with an arbitrary small amplitude as starting condition X^0 for the initial value code. To be consistent with the linear stability approach we take $NF=1$ and compute the value of a velocity component as a function of time, e.g., $u_r(x=0.5,\ \zeta=0, t)$. The growth rate $\sigma=1/(t_2-t_1)\log_e u_r(t_2)/u_r(t_1)$ between two arbitrary times t_1 and t_2 is calculated and compared to σ_0. Some results are shown in Table I: the relative difference $\delta\sigma=(\sigma-\sigma_0)/\sigma_0$ is about $10^{-5}\%$ at the smallest time step $\Delta t=10^{-4}$ used. Note that $\delta\sigma$ scales with $(\Delta t)^2$. We now make a comparison with published work. Krueger *et al.* [21] reported that at $\eta=0.95$ steady Taylor vortices onset at wavenumber $\alpha=3.128$ and Taylor number $Ta=-4a\Omega_1\delta^4/\nu^2=3509.9$. For parameters of these values our linear stability code finds that the growth rate is indeed close to zero, $\sigma_0=-0.7017\times10^{-3}$. The initial value code gives the same growth rate, the relative difference being only 0.04%. Another test is the comparison with Marcus [17]; at $\eta=0.5$, $\alpha=3.161$, and steady Reynolds number $\mathrm{Re}_1=74.924$ he found the growth rate $\sigma_A=0.035637$ using a fourth-order solver and $\sigma_B=+0.035636$ using his initial value code. For parameters of these values both our linear stability code and the initial value code give, after conversion into Marcus' dimensionless units, $\sigma=0.035639$, with a relative difference of only 0.008% from σ_B and 0.006% from σ_A.

(2) *Steady state Taylor vortex flow and convergence in NC and NF.* We compute the nonlinear steady state Taylor vortex flow and compare the results with the published values of Jones [15]. Useful measures of the strength of the vortices are the radial velocity components u_r and the torques G_1 and G_2 on the inner and outer cylinder, given by

$$G_1=\frac{-2(1+\xi)}{\eta(1+\eta)}+\frac{1}{(\overline{\mathrm{Re}}_1-\eta\,\overline{\mathrm{Re}}_2)}\frac{\partial v}{\partial x}(x=0) \tag{3.14}$$

$$G_2=\frac{-2(1+\xi)}{\eta(1+\eta)}+\frac{1}{\eta^2}\frac{1}{(\overline{\mathrm{Re}}_1-\eta\,\overline{\mathrm{Re}}_2)}\frac{\partial v}{\partial x}(x=1), \tag{3.15}$$

where $\xi=[\overline{\mathrm{Re}}_1\varepsilon_1\sin(\omega_1 t)-\eta\overline{\mathrm{Re}}_2\varepsilon_2\sin(\omega_2 t)]/\overline{\mathrm{Re}}_1-\eta\overline{\mathrm{Re}}2)$. G_1 and G_2 have the same magnitude. To obtain the dimensional torques from (3.15) and (3.16) one multiplies G_1 and G_2 times $2\pi h\nu\rho(\bar{\Omega}_1-\bar{\Omega}_2)\,R_1^3\delta$, where h is the length of the cylinders. Table II shows steady state values of u_r, G_1, and G_2 as a function of increasing number of Chebyshev polynomials *NC* and Fourier terms *NF*. The results converge towards the values reported by Jones. Note that G_1 is different from G_2, but $(G_1-G_2)/G_1$ becomes smaller if more Chebyshev polynomials are used to take care of the asymmetry between the flow at the inner and at the outer boundaries. The asymmetry becomes less in the narrow gap limit $\eta\to1$ (in the present test $\eta=0.5$). At higher values of Reynolds number more polynomials and Fourier terms are needed to obtain the same accuracy and to represent the increasing asymmetry between the outflow and the inflow at $\zeta=0$ and $\zeta=2\pi/\alpha$. Fortunately the phenomena we are interested in happens at moderate Reynolds numbers, around $\mathrm{Re}_{10}(1+\varepsilon_1)$, where $\varepsilon_1<1$, and so we never need a high number of polynomials.

TABLE II

The radial Velocity u_r at the Point $x=0.5$, $\zeta=0$ and the Magnitude of the Torques G_1 and G_2 on the Inner and Outer Cylinders

Ta	NC	NF	u_r	G_1	G_2	$(G_1-G_2)/G_1$
3500	7	3	4.264242	2.805078	2.809117	1.44×10^{-3}
3500	13	5	4.233583	2.812993	2.813026	1.15×10^{-5}
3500	13	7	4.233625	2.812993	2.813026	1.15×10^{-5}
3500	13	9	4.233625	2.812993	2.813026	1.15×10^{-5}
3500	15	5	4.233584	2.813015	2.813019	1.87×10^{-6}
3500	15	7	4.233584	2.813015	2.813010	1.87×10^{-5}
3500	15	9	4.233626	2.813015	2.813010	1.87×10^{-6}
7500	10	4	17.832047	3.591168	3.609267	5.04×10^{-3}
7500	12	4	17.832587	3.586544	3.585045	4.18×10^{-4}
7500	15	4	17.832865	3.586549	3.586517	8.98×10^{-6}
7500	15	8	17.969645	3.587657	3.587622	9.83×10^{-6}
7500	15	10	17.970411	3.587657	3.587622	9.83×10^{-6}
15000	12	4	33.644945	4.158712	4.167972	2.23×10^{-3}
15000	15	4	33.643340	4.155552	4.153110	5.88×10^{-4}
15000	15	8	33.656768	4.186246	4.183858	5.70×10^{-4}
15000	15	10	33.677391	4.186250	4.183863	5.70×10^{-4}

Note. Computed by means of the initial value code at $\eta=0.5$, $\alpha=3.1631$, $\mu=0$, and Taylor numbers 3500 ($\mathrm{Re}_1\approx72.5$), 7500 ($\mathrm{Re}_1\approx106.1$), and 15,000 ($\mathrm{Re}_1=150$) at different truncation NC and NF of Chebyshev polynomials and Fourier terms. Jones' results [15] are: $u_r=4.23363$ and $G=2.813015$ at $Ta=3500$; $u_r=17.9705$ and $G=3.5878$ at $Ta=7500$; $u_r=33.6805$ and $G=4.1864$ at $Ta=15{,}000$.

It is interesting to look at the contribution of the various Fourier components $u_r^m(x)$ to the total radial velocity $u_r(x,\zeta)=\sum_{m=1}^{m=NF}u_r^m(x)\cos(m\alpha\zeta)$ for a typical steady state Taylor vortex flow: in Fig. 1 one verifies that u_r^m drops smoothly over orders of magnitude from $m=1$ to $m=NF$ inclusive. We do not apply any corrections for aliasing effects.

(3) *Viscous wave.* At low enough Reynolds number the solution of the Navier–Stokes equations (2.6) to (2.9) has only an azimuthal velocity component, which can be easily calculated. Let the velocities of the cylinder be $V_i(t)=R_i[\bar{\Omega}_i+A_i\cos(\omega t)]$, $i=1,2$. Then the total azimuthal velocity is $V(r,t)=V_0(r)+u(r,t)$, where $V_0(r)$ is the mean Couette flow $V_0(r)=\bar{A}r+\bar{B}/r$ (the overbar indicates the time average) and

$$u(r,t)=\mathrm{Real}[\{R_1A_1[I_1(x_2)K_1(x)-K_1(x_2)I_1(x)]/\Delta + R_2A_2[K_1(x_1)I_1(x)-I_1(x_1)K_1(x)]/\Delta\}e^{i\omega t}], \tag{3.17}$$

where $x=e^{i\pi/4}\sqrt{\omega/\nu}\,r$ and $\Delta=K_1(x_1)I_1(x_2)-K_1(x_2)I_1(x_1)$. $K_1(x)$ and $I_1(x)$ are the modified Bessel functions of the first kind. The initial value code can reproduce this time dependent flow well; we choose $\eta=0.5$, $\alpha=3.1631$, and modulation with

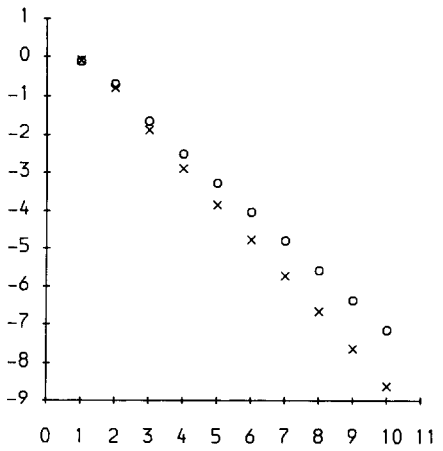

FIG. 1. Relative intensity $\log_{10} u_r^m/u_{ro}$ of the Fourier component u_r^m of u_r as a function of m, calculated at the point $x = 0.5$, $\zeta = 0$ at $\delta/R_1 = 0.444$, $\alpha = 3.13$, with $NC = 15$ and $NF = 10$. *Crosses*: steady state flow at $\mathrm{Re}_1 = 86.025731$; $u_{ro} = 5.6385$ is the steady state radial velocity. *Circles*: modulated flow at $\overline{\mathrm{Re}}_1 = 86.025731$, $\varepsilon_1 = 0.3$, and $T_1 = 0.5$ computed with $N_T = 1250$; $u_{ro} = 9.9028$ is the peak radial velocity during a cycle.

$\overline{\mathrm{Re}}_1 = 40$, $\varepsilon_1 = 0.5$, and $T_1 = 2$. With $NC = 16$ Chebyshev polynomials and $\Delta t = 10^{-3}$ we find that at the point $x = 0.5$ the initial value code agrees with the exact solution within 10^{-4}–10^{-5}%.

(4) *Modulated Taylor–Couette flow: Convergence in Δt, NC and NF.* We choose Carmi and Tustaniwskyj's radius ratio [6] given by $\delta/R_1 = \eta/(1-\eta) = 0.444$, and consider oscillations at $\overline{\mathrm{Re}}_1 = 86.025731$, $\varepsilon_1 = 0.3$ with period $T_1 = 1.5$ and wavenumber $\alpha = 3.13$. We examine the convergence in Δt at fixed $NC = 10$ and

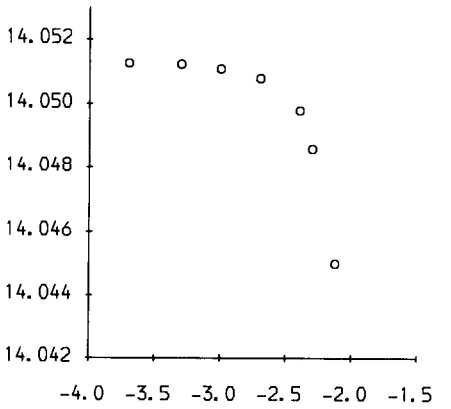

FIG. 2. Maximum value of u_r during a cycle as a function of $\log_{10} \Delta t$, where Δt is the time step calculated at the point $x = 0.5$, $\zeta = 0$ with fixed $NC = 10$ and $NF = 6$. The oscillations are at $\delta/R_1 = 0.444$, $\alpha = 3.13$, $\overline{\mathrm{Re}}_1 = 86.025731$, $\varepsilon_1 = 0.3$, and $T_1 = 1.5$.

TABLE III

Oscillations at $\delta/R_1 = 0.444$, $\alpha = 3.13$, $\overline{\mathrm{Re}}_1 = 86.025731$, $\varepsilon_1 = 0.3$, and $T_1 = 1.5$

NC \ NF	4	5	6	7	8	9
8	13.9906	14.0143	14.0199	14.0211	14.0214	14.0214
9	14.0163	14.0414	14.0473	14.0486	14.0489	14.0489
10	14.0206	14.0454	14.0511	14.0524	14.0526	14.0527
12	14.0192	14.0439	14.0496	14.0509	14.0511	14.0512
13	14.0193	14.0441	14.0498	14.0510	14.0513	14.0513
14	14.0193	14.0440	14.0497	14.0510	14.0513	14.0513
15	14.0193	14.0440	14.0497	14.0510	14.0513	14.0513

Note. The maximum value of u_r during a cycle is calculated at the point $x = 0.5$, $\zeta = 0$ at the fixed time step $\Delta t = 0.001$ as a function of the number of Chebyshev polynomials NC and Fourier terms NF.

$NF = 6$. The results for the peak value of the radial velocity during an oscillation at the point $x = 0.5$, $\zeta = 0$ are summarised in Fig. 2. The two entries at the smallest time steps $u_r = 14.05124$ and $u_r = 14.05127$ differ by only 0.0002%. To study the convergence as a function of NC and NF we keep $\Delta t = 10^{-3}$ fixed; the results are showed in Table III.

In our previous paper [3] we have shown that calculations of velocity components as a function of time have very good quantitative agreement with the measurements of Ahlers [10] and reproduce the characteristic unharmonic shapes.

4. The Floquet Theory

In this section we describe the Floquet theory which we use to determine the stability of Taylor–Couette flow. Floquet theory is essentially a linear stability theory for an unperturbed state which is periodic in time. Let U_i $(i = 1, ..., N)$ be a set of N modes which represent independent perturbations from the oscillatory state. These modes are orthogonal and normalized and form a complete set, in the sense that any state of the system can be uniquely described by the U_i. We integrate each mode $U_i = U_i(0)$ from time $t = 0$ to $t = T$, the period of an oscillation. By expanding each final mode $U_i(T)$ over the original set $\{U_i(0)\}$ we construct the matrix C:

$$U_j(T) = \sum_{i=1}^{i=N} C_{ji} U_i(0) \qquad (j = 1, ..., N). \tag{4.1}$$

Let us assume that there is a solution of the form $\Psi(t) = e^{\sigma t} F(t)$, where F is periodic, i.e., $F(0) = F(T)$. Then $\Psi(T) = e^{\sigma T} \Psi(0)$. We expand $\Psi(t)$ over the set

$\{U_j\}$; we have $\Psi(0)=\Sigma_j b_j U_j(0)$ and $\Psi(T)=\Sigma_j b_j U_j(T)=\Sigma_j\Sigma_i b_j C_{ji} U_i(0)$. Since $\Psi(T)=e^{\sigma T}\Sigma_i b_i U_i(0)$, we obtain $\Sigma_i U_i(0)[b_i e^{\sigma T}-\Sigma_j b_j C_{ji}]=0$. But $\{U_i(0)\}$ form a complete set; we have $b_i e^{\sigma T}-\Sigma_j b_j C_{ji}=0$ for each i. If we introduce the transposed matrix $D=C'$, the vector $B=(b_1, ..., b_N)$ and the unit matrix I we can write $(D-e^{\sigma T}I)\,B=0$. A nontrivial solution exists if $\det(D-e^{\sigma T}I)=0$. This relation determines N eigenvalues. The growth rate is $\sigma=(1/T)\log_e \Lambda$ where Λ is the largest eigenvalue. If $|\Lambda|>1$ then modulated Couette flow is unstable.

We implement the Floquet theory in the following way. We recall that the state of the system is described by a vector X containing the Chebyshev–Fourier coefficients of the expansions of Z, v, and Ψ. Since we are interested in a linear theory we take $NF=1$ in these expansions. Let the perturbation of the azimuthal velocity v be

$$\delta v_n = T^*_{n-1}(x) - T^*_{n+1}(x) \qquad (n=1, ..., NC-2). \tag{4.2}$$

These $NC-2$ independent modes form a complete set in the space of functions $S_1=\{f(x)$ such that $f(x)=\sum_{j=1}^{j=NC} f_j T^*_{j-1}(x)$ and $f(0)=f(1)=0\}$ to which v belongs. We make the modes δv_n orthogonal by means of the Gram–Schmidt procedure and then normalize them. To do this we need to define the inner product (f, g) in S_1. We have

$$(f, g)=\sum_{n=1}^{n=M}\sum_{m=1}^{m=N} f_n g_m (T^*_{n-1}, T^*_{m-1}) = \sum_{n=1}^{n=M}\sum_{m=1}^{m=M} f_n g_m h_{m-1}, \tag{4.3}$$

since $(T^*_n, T^*_m)=\int_{x=0}^{x=1} dx\,(x-x^2)^{-1/2}\,T^*_n(x)\,T^*_m(x)=\delta_{nm}h_n$, where $h_n=\pi/2$ if $n=0$ and π otherwise. We call $U^v_n(x)$ $(n=1, ..., NC-2)$ the set of resulting perturbations of v for which $(U^v_n, U^v_m)=\delta_{nm}$.

The perturbations of the stream function are

$$\delta\Psi_n(x)=T^*_{n-1}(x)+c_1 T^*_{n+1}(x)+c_2 T^*_{n+3}(x) \qquad (n=1, ..., NC-2) \tag{4.4}$$

with

$$c_1=\frac{(n-1)^2-(n-3)^2}{(n+3)^2-(n+1)^2}, \qquad c_2=\frac{(n+1)^2-(n-1)^2}{(n+3)^2-(n+1)^2} \tag{4.5}$$

These $NC-2$ independent modes are a complete set in the space of functions $S_2=\{f(x)$ such that $f(x)=\sum_{j=1}^{j=NC+2} f_j T^*_{j-1}(x)$ and $f(0)=f(1)=(df/dx)(0)=(df/dx)(1)=0\}$ which we use to describe Ψ. Proceeding in the same way as we did for δv_n we construct the functions $U^\Psi_n(x)$ $(n=1, ..., NC-2)$ such that $(U^\Psi_n, U^\Psi_m)=\delta_{nm}$. Note that for each of the perturbations of $\delta\Psi_n(x)$ we have to adjust the vorticity according to (2.8) by computing the corresponding $\delta Z_n(x)$.

We use a linearized version of the initial value code described in Section 3 to integrate each of the $(NC-2)+(NC-2)$ perturbations U^v and U^Ψ in time from $t=0$ to $t=T$. The coefficients of v and Ψ in the final state vector X are then used to construct the matrix D. The largest eigenvalue Λ of D, obtained by means of a

TABLE IV

The Growth Rate σ Computed by Means of the Floquet Theory Code as a Function of the Time Step Δt and the Total Number of Steps N_T at $\delta/R_1 = 0.444$, $\alpha = 3.13$. $\mathrm{Re}_1 = 80$ with $NC = 15$ Chebyshev Polynomials

Δt \ N_T	50	100	200	1000	2000
0.01	3.24×10^{-1}	1.91×10^{-1}	1.24×10^{-1}	7.07×10^{-2}	6.41×10^{-2}
0.005	1.48×10^{-1}	8.10×10^{-2}	4.79×10^{-2}	2.11×10^{-2}	1.77×10^{-2}
0.001	2.74×10^{-2}	4.40×10^{-2}	7.28×10^{-3}	1.92×10^{-3}	1.25×10^{-3}
0.0001	2.72×10^{-3}	1.36×10^{-3}	6.79×10^{-4}	1.42×10^{-4}	7.30×10^{-5}

Note. The tabulated results are in the form $(\sigma - \sigma_0)/\sigma_0 \times 100$, where $\sigma_0 = 0.430108693$ was obtained by means of the steady state linear stability code.

NAG routine, determine the stability of the flow. A number of checks of the Floquet theory have been performed:

(1) *Steady state problem.* We use the known results about the stability of steady Taylor–Couette flow to test the Floquet theory code: we set T equal to an arbitrary time $T = N_T \Delta t$ and compute the growth rate σ. At $\delta/R_1 = 0.444$, $\alpha = 3.13$, and $\mathrm{Re}_1 = 80$ the steady state linear stability program mentioned in Section 3 gives $\sigma_0 = 0.430108693$. The results of the Floquet theory at $NC = 15$ are shown in Table IV as a function of the time step Δt and the total number of steps N_T. The agreement is good: $\sigma \to \sigma_0$ at large N_T. The last two entries at the smallest Δt differ by only $7.2 \times 10^{-5}\%$.

(2) *Modulated case, convergence as a function of NC and Δt.* We study Taylor–Couette flow modulated at $\overline{\mathrm{Re}}_1 = 78$, $\varepsilon_1 = 0.5$ at the same radius ratio and wavenumber as before. The largest eigenvalue Λ is computed as a function of the number NC of Chebyshev polynomials and time step Δt. The results corresponding to two choices of the period of oscillation $T_1 = 0.125$ and $T_1 = 1.5$ are shown in Table V and VI. From the entries with the smallest Δt one can see that halving the

TABLE V

The Largest Eigenvalue Λ Computed by Means of the Floquet Theory Code

NC \ N_T	100	200	400	800	1600	3200
10	0.98533	0.98589	0.98502	0.98606	0.98607	0.98607
14	0.98533	0.98589	0.98602	0.98606	0.98607	—
18	0.98533	0.98589	0.98602	0.98606	0.98607	—

Note. $\delta/R_1 = 0.444$, $\alpha = 3.13$, $\overline{\mathrm{Re}}_1 = 78$, $\varepsilon_1 = 0.5$, $T_1 = 0.125$ as a function of the number of Chebyshev polynomials NC and the number of time steps in a cycle N_T.

TABLE VI

The same as in Table V but $T_1 = 1.5$

NC \ N_T	100	200	400	800	1600	3200
8	0.9709	0.9879	0.9922	0.9933	0.9936	0.9936
10	0.9700	0.9869	0.9912	0.9923	0.9926	0.9926
14	0.9700	0.9869	0.9912	0.9923	0.9926	—
18	0.9700	0.9869	0.9912	0.9923	—	—

time step causes a change of Λ of only 0.0001% at the higher frequency T_1. At the lower frequency T_2 the corresponding change is 0.0005%.

We have mentioned in the Introduction that the Floquet theory gives results different from Carmi and Tustaniwskyj's [6]. They examined oscillations with amplitude $\varepsilon_1 = 0.5$ and wavenumber $\alpha = 3.13$ at radius ratio given by $\delta/R_1 = 0.444$; at their lowest frequency ($\omega_1 = 2$) they predicted $r = (\overline{\mathrm{Re}}_{1C} - \overline{\mathrm{Re}}_{10})/\overline{\mathrm{Re}}_{10} = -30.6\%$, while we find only $r = -0.8\%$. To understand this order-of-magnitude disagreement we investigate at first the effect of severe mode truncation in our numerical code, because Carmi and Tustaniwskyj employed typically only three or four Galerkin modes in their calculation while we use $NC = 15$ Chebyshev polynomials. At $\omega_1 = 2$, with decreasing $NC = 7$, 6, 4, and 3, we obtain respectively $\overline{\mathrm{Re}}_{1C} = 78.05$, 77.88, 78.45, and 71.67 which should be compared with the critical Reynolds number for the onset of vortices in the steady state problem $\mathrm{Re}_{10} = 78.7173$. We con-

TABLE VII

Effect of Increasing the Time Step

ω_1	N_T	$\overline{\mathrm{Re}}_{1C}$
200	1000	78.63
200	500	78.63
200	100	78.64
200	60	78.67
200	30	78.77
2	1600	78.02
2	800	78.06
2	60	42.06
2	30	23.90

Note. Critical Reynolds number $\overline{\mathrm{Re}}_{1C}$ for modulated flow at $\delta/R_1 = 0.444$, $\varepsilon_1 = 0.5$ as a function of number N_T of steps per cycle at various frequencies ω_1. $NC = 15$ Chebyshev polynomials have been used.

clude that the reduction of the number of modes fails to reproduce Carmi and Tustaniwskyj's large destabilisation. We then turn our attention to the time stepping. Carmi and Tustaniwskyj introduced a scaled time $\tau = \omega_1 t$ and performed the time integration with $N_T = 30$ steps per cycle, where $N_T = T_1/\Delta t$. We examine the effect of running our numerical code with a time step much larger than discussed in our previous tests of convergence. The results are shown in Table VII. At high frequency of modulation ($\omega_1 = 200$) the small number N_T of steps per cycle used by Carmi and Tustaniwsky gives a fair result. However, to achieve convergence at low frequency of modulation ($\omega_1 = 2$), we need a much bigger N_T; if N_T is too small, a large bogus reduction of the critical Reynolds number is obtained, comparable to the reduction reported by Carmi and Tustaniwskyj. This bogus effect arises because at low frequency of modulation the amplitude falls to very low values during part of the cycle; with a large time step the numerical solution "jumps" across this part of the cycle too fast and fails to compute the very small velocity with enough accuracy. On the contrary, at high frequency of modulation, the amplitude does not fall to small values and the problem does not occur. We suspect that Carmi and Tustaniwskyj checked the time step at high frequency only and were misled by the result and by their introduction of a dimensionless time scaled with the frequency.

5. Applications of the Initial Value Code to Stretched Taylor Vortices

In Section 2 we have mentioned that the axial wavenumber α has the typical value 3.13 in both steady and modulated Taylor vortex flow. It is possible, however, to stretch the vortices by a considerable amount so that α becomes much less than 3.13; to achieve this result, for example, the experimenter can slowly move the end cap which limits the height of the Couette apparatus while some new fluid enters the gap [22]. To illustrate an application of the initial value code we present some new results about stretched Taylor vortices.

An oscillation of the whole vortex pattern between wavenumbers α and 2α is possible if during the initial part of the cycle, when the Reynolds number is high, a vortex pair breaks into two pairs, while during the final part of the cycle the vortices merge. This pattern oscillation is a clean way of studying both numerically and experimentally the detailed development of a Taylor cell because it does not depend on noise [23] or complicated end effects. We choose wavenumber $\alpha = 2.5$ at radius ratio $\eta = 0.5$, and examine modulation with aplitude $\varepsilon_1 = 0.7$ around the mean value $\overline{\mathrm{Re}}_1 = 78$. The steady state linear stability theory predicts that vortices with wavenumbers α and 2α onset respectively at $\mathrm{Re}_{10} = 70.72$ and 80.25. We expect to see an oscillation of the vortex pattern if the frequency of modulation is slow enough and assume $T_1 = 6$. If the frequency is too high, in fact, there is not enough time for the vortices to respond to the change in Reynolds number. The details of the vortex pair formation can be seen in Fig. 3a to 3*j*, where contour plots of the potential vorticity Z are displayed at successive times t during the part of the cycle in which the transition from wavenumber α to 2α takes place.

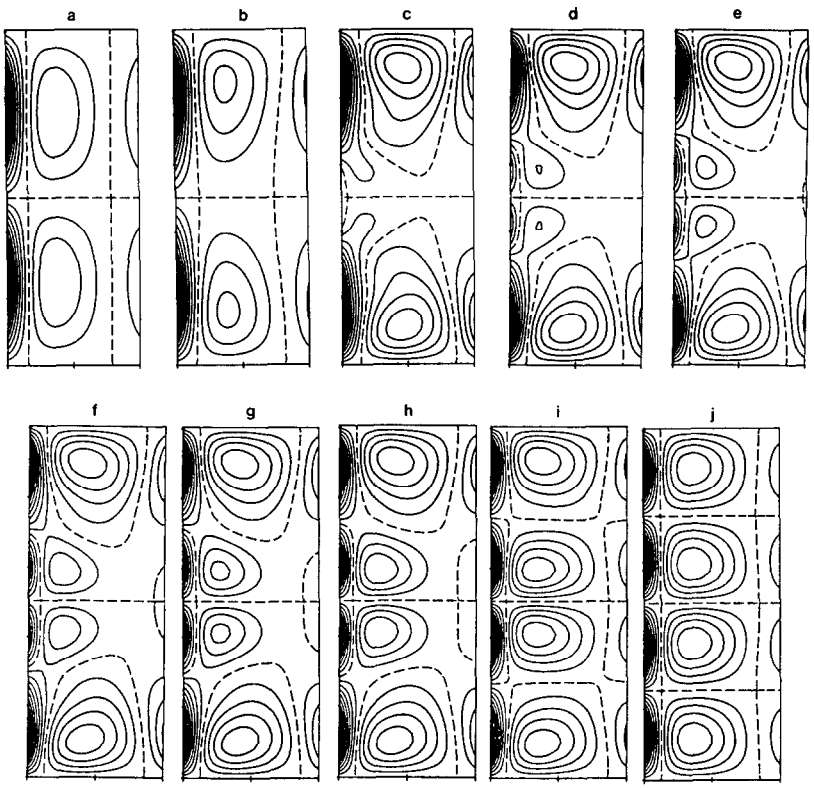

FIG. 3. Modulation of stretched vortices with wavenumber $\alpha = 2.5$ at $\eta = 0.75$, $\varepsilon_1 = 0.4$, $\overline{\mathrm{Re}}_1 = 78$, and $T_1 = 6$. Sequence of contour plots of the potential vorticity Z at different times t during the formation of a new vortex pair. The calculation is performed with $NC = 15$, $NF = 4$, and $N_T = 6000$. The contour heights are $\Delta Z = Z_{\max}/10$. The dotted line is the zero height: (a) $t = 1.6$, $\mathrm{Re}_1 = 109.03$, $Z_{\max} = 12.7$; (b) $t = 1.75$, $\mathrm{Re}_1 = 108.14$, $Z_{\max} = 280$; (c) $t = 1.85$, $\mathrm{Re}_1 = 107.13$, $Z_{\max} = 493$; (d) $t = 2.03$, $\mathrm{Re}_1 = 104.52$, $Z_{\max} = 452$; (e) $t = 2.06$, $\mathrm{Re}_1 = 103.99$, $Z_{\max} = 449$; (f) $t = 2.09$, $\mathrm{Re}_1 = 103.43$, $Z_{\max} = 449$; (g) $t = 2.12$, $\mathrm{Re}_1 = 102.85$, $Z_{\max} = 450$; (h) $t = 2.15$, $\mathrm{Re}_1 = 102.25$, $Z_{\max} = 454$; (i) $t = 2.25$, $\mathrm{Re}_1 = 100.06$, $Z_{\max} = 443$; (j) $t = 3$, $\mathrm{Re}_1 = 78$, $Z_{\max} = 137$.

At the beginning of the cycle the Taylor cell remains symmetric for a while (Fig. 3a) because the vortices lag behind the drive. Then (Fig. 3b) the vortex cores and the layers of high vorticity close to the inner wall move away from the centre of the cell towards the outflow regions. The layers develop intrusions which extend towards the centre of the cell (Fig. 3c). Because of the progressive growth of a small patch of vorticity near the inflow, the intrusions make necks (Fig. 3d, e) and eventually break away as new vortex cores (Fig. 3f). At first the new cores are smaller and closer to the inner cylinder than the original cores (Fig. 3g), but then they grow in size until the vortices reach their maximum strength (Fig. 3h, i). During the decay the pattern settles into its new symmetry (Fig. 3j). As the Reynolds number decreases the vortices weaken, until the reverse transition from 2α to α takes place

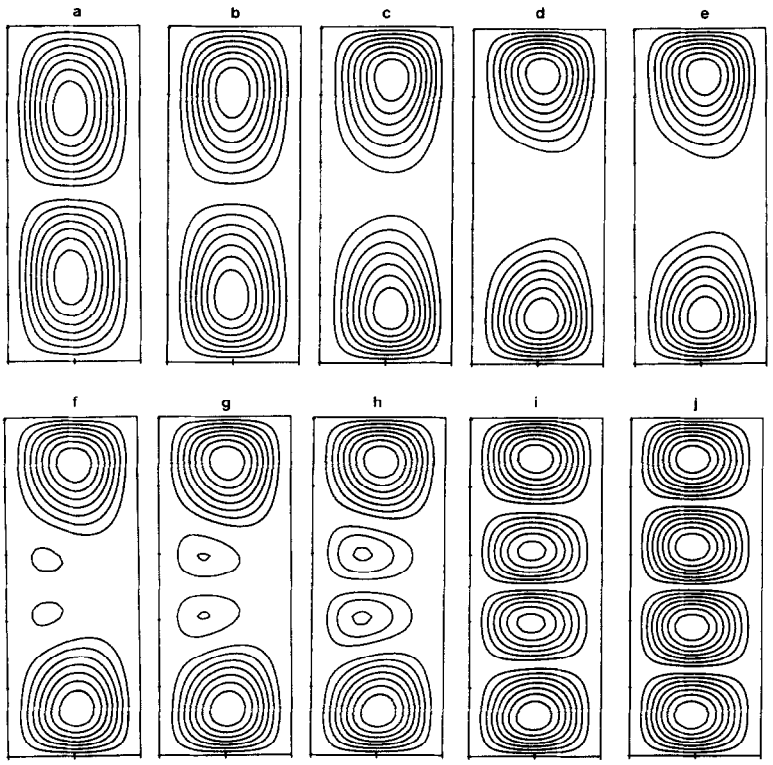

FIG. 4. Sequence of countour plots of the stream function Ψ as in Fig. 3. The contour heights are $\Delta\Psi = \Psi_{max}/8$: (a) $\Psi_{max} = 0.082$; (b) $\Psi_{max} = 1.88$; (c) $\Psi_{max} = 4.44$; (d) $\Psi_{max} = 3.64$; (e) $\Psi_{max} = 3.53$; (f) $\Psi_{max} = 3.39$; (g) $\Psi_{max} = 3.39$; (h) $\Psi_{max} = 3.24$; (i) $\Psi_{max} = 3.11$; (j) $\Psi_{max} = 2.64$.

and the vortices merge together. The same temporal sequence is shown in Fig. 4a to 4j to illustrate the behaviour of the stream function φ.

We have also found that temporally modulated stretched vortices exhibit subharmonic response. To examine this effect it is convenient to monitor the time dependence of the sign of u_r computed at the point $x = 0.5$, $\zeta = 0.5\lambda$, where $\lambda = 2\pi/\alpha$ is the cell wavelength. This point lies on the inflow and u_r is negative, but if the cell breaks and the wavenumber becomes 2α then the point is on the outflow and u_r becomes positive. We choose the parameters $\alpha = 2.5$, $\eta = 0.5$ and modulate the Reynolds number with $\varepsilon_1 = 0.4$, $\overline{\mathrm{Re}}_1 = 78$, and period $T_1 = 6$. Figure 5 shows that the stretched Taylor vortices respond subharmonically with period $2T_1$: the vortex cell breaks every other cycle, as evident from the change in sign of u_r; during the first cycle displayed in the figure (from $t = 0$ to $t = 6$) the Taylor vortices do not break and u_r is always negative; during the second cycle (from $t = 6$ to $t = 12$) the transition from α to 2α takes place and u_r becomes positive. During the final part of the second cycle the vortices weaken until they merge together at $t \approx 10$ and u_r becomes negative again (its value is too small to be seen in the figure). This

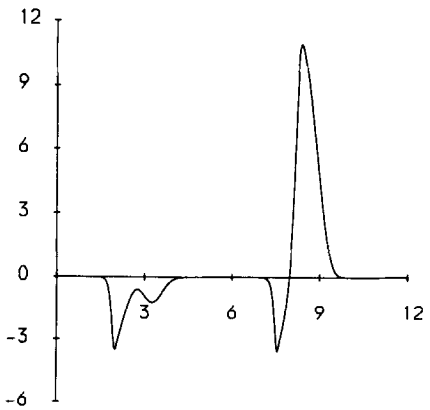

FIG. 5. Subharmonic response of stretched vortices with $\alpha = 2.5$ at $\eta = 0.5$, $\varepsilon_1 = 0.4$, $\overline{\mathrm{Re}}_1 = 78$, and $T_1 = 6$; plot of u_r vs time at the point $x = 0.5$, $\zeta = 0.5\lambda$ with $NC = 15$, $NF = 8$, and $N_T = 6000$.

behaviour is found to be stable in time and the calculation was repeated at different values of truncation NC and NF and at different number N_T of time steps per cycle ($NC = 10$, $NF = 4$, $N_T = 3000$; $NC = 15$, $NF = 4$, $N_T = 3000$ and 12,000; $NC = 15$, $NF = 8$, $N_T = 6000$). It is also found that the subharmonic response exists only if the frequency of modulation is slow enough: at the same parameters of Fig. 5 the effect disappears if the period of modulation is $T_1 = 4$.

Close inspection of the value of u_r shows that at the end of the first cycle (in which the vortices break) we have $u_r = -0.8 \times 10^{-7}$ at $t = T_1 = 6$ and $u_r = -0.3 \times 10^{-7}$ at $t = 2T_1 = 12$. As a consequence the peak in the second oscillation rises sooner than in the first one, and the vortex has time to break before the Reynolds number decreases again. The values of u_r at the beginning of each cycle are orders of magnitude above the numerical noise but they are very small. It is therefore possible that the subharmonic response exists only within the frame of the perfect bifurcation, as represented by the calculation; in the experiments, as discussed in Ref. [3], small imperfections in the transition region when $u_r \approx 0$ have important consequences at low frequency modulation, and they may destroy the subharmonic effect if this is very sensitive to the precise value of u_r at the beginning of each cycle. In any case, Fig. 5 shows the interesting fact that two different solutions for the flow are possible.

ACKNOWLEDGMENTS

The author is indebted to Dr. C. A. Jones for help and discussion during this work and wishes to thank Professors G. Ahlers and R. J. Donnelly for access to unpublished data. The support of SERC Grant GR/D30433 is acknowledged.

REFERENCES

1. S. H. DAVIS, *Ann. Rev. Fluid Mech.* **8**, 57 (1976).
2. R. J. DONNELLY, *Proc. Roy. Soc. London A* **781**, 130 (1964).
3. C. F. BARENGHI AND C. A. JONES, *J. Fluid Mech.* **208**, 127 (1989).
4. R. THOMSON, Ph.D. thesis, Dept. of Meteorology, Massachusetts Institute of Technology, 1969 (unpublished).
5. T. J. WALSH AND R. J. DONNELLY, *Phys. Rev. Lett.* **58**, 2543 (1988).
6. S. CARMI AND J. I. TUSTANIWSKYJ, *J. Fluid Mech.* **108**, 19 (1981); J. I. TUSTANIWSKYJ AND S. CARMI, *Phys. Fluids* **23**, 1732 (1983).
7. P. HALL, *J. Fluid Mech.* **67**, 29 (1975); **126**, 357 (1983).
8. P. J. RILEY AND R. L. LAURENCE, *J. Fluid Mech.* **79**, 535 (1977).
9. H. KUHLMANN, D. ROTH, AND M. LUCKE, *Phys. Rev. A* **39**, 745 (1988).
10. G. AHLERS, Physics Dept., University of California at Santa Barbara, private communication (1988).
11. T. J. WALSH AND R. J. DONNELLY, *Phys. Rev. Lett.* **60**, 700 (1988).
12. K. A. MEYER, *Phys. Fluids Suppl. II* **12**, 165 (1969).
13. E. H. ROGERS AND D. W. BEARD, *J. Comput. Phys.* **4**, 1 (1969).
14. R. MEYER-SPASCHE AND H. B. KELLER, *J. Comput. Phys.* **35**, 100 (1980).
15. C. A. JONES, *J. Comput. Phys.* **61**, 321 (1985).
16. R. D. MOSER, P. MOIN, AND A. LEONARD, *J. Comput. Phys.* **52**, 524 (1983).
17. P. S. MARCUS, *J. Fluid Mech.* **146**, 45 (1984).
18. S. A. ORSZAG AND A. T. PATERA, *J. Fluid Mech.* **128**, 347 (1983).
19. D. GOTTLIEB AND S. A. ORSZAG, *Numerical Analysis of Spectral Methods* (SIAM, Philadelphia, 1971).
20. C. F. BARENGHI AND C. A. JONES, *J. Fluid Mech.* **197**, 552 (1988).
21. E. R. KRUEGER, A. GROSS, AND R. C. DIPRIMA, *J. Fluids Mech.* **24**, 521 (1966).
22. H. A. SNYDER, *J. Fluids Mech.* **35**, 337 (1969).
23. J. C. CHEN, G. P. NEITZEL, AND D. F. JANKOWSKI, *Phys. Fluids* **30**, 1250 (1987).